Quasi-stationary numerical model of the dielectric barrier discharge

M.R. Ghazanchaei, K. Adamiak, G.S.P. Castle
Dept. of Electrical & Computer Engineering
University of Western Ontario
e-mail: mghazanc@uwo.ca

Abstract— **The aim of this study is to present a numerical algorithm for investigating the dynamic characteristics of simple model of dielectric barrier discharge (DBD) in air. The proposed algorithm is based on the finite element method (FEM) and is capable to determine the distribution of electric field intensity and space charge density in the point to plane geometry when the plane is covered with a thin dielectric layer and the needle is energized with a sinusoidal voltage. The simulation results show the behavior of corona current and space charge density under the imposed voltage. The simulations were performed for a few values of the input voltage and frequency. The aim of this parametric study is to investigate the effect of voltage, and frequency on the time variation of the discharge.**

Keywords- dielectric barrier discharge (DBD), finite element method (FEM), transient simulation, current, space charge density

I. INTRODUCTION

The dielectric barrier discharge (DBD) is used in various important applications, such as ozone generation, pollution control, electrostatic precipitation, fluid flow control and many other industrial processes. This discharge is closely related to corona discharge (CD). Both discharges have common features such as the strong influence of the local field distortions caused by space charge distribution [1]. Although, the electric field established by the electrodes in corona discharge can be produced by dc voltage, ac voltage, or pulse voltage, a dielectric barrier discharge requires alternating voltages for its operation [2]. The dielectric layer deposited on one or both electrodes cannot pass a dc current. Its electric permittivity and thickness, in combination with the time derivative of the applied voltage, dV/dt determine the amount of displacement current that can be passed through the dielectric [2]. Barrier discharges can be operated in various modes (e.g., diffuse, patterned, filamentary, micro discharge), and the terminology can often become confusing [3]. At atmospheric pressure, electrical breakdown in a large number of micro discharges is the normal situation for most gases in DBD. Under certain circumstances it is possible to obtain apparently homogeneous, diffuse discharges [4], or regularly spaced glow discharge patterns [5]. At lower pressure, diffuse glow discharges can always be obtained [3].

One interesting application of DBD is in an electrostatic precipitator (ESP) [6]. Electrical behavior of the precipitator has been investigated in an experimental set up, and the current waveform of the discharge was recorded. Effects of voltage and AC frequency on the extent and propagation velocity of the discharge have been investigated experimentally. Sensitivity analysis showed that the particle collection efficiency of the ESP increases with the applied voltage. However, it depends on the frequency and for both low and very high frequency the precipitation efficiency decreases. A few geometric and parametric studies have been done in order to investigate the effect of discharge channel geometry. Studies were carried out for different thicknesses, lengths and numbers of tubes. The dissipated power has been calculated in the system. Although these results look promising, there is no equivalent circuit model or numerical algorithm presented in this study and all the works are based on experimental results [7]. Very little work has been carried out in order to analyze the effect of the ionic wind on the particle collection efficiency, and to investigate the correlation between the EHD flow and the collection efficiency [8]. The effects of the geometry of the dielectric barrier discharge have been investigated by a few authors [9]. Despite these widespread applications, there is no reliable and accurate numerical model for the computer simulation of this phenomenon. A few numerical techniques for modeling DBD have been reported in the literature and they vary either with respect to the applications or the memory requirements, computation speed and accuracy. A 1D model for the DBD has been developed based on the numerical solution of the electron and ion continuity and momentum transfer equations coupled to Poisson's equation [10]. This model gave space and time variations in the electric field, and the electron and ion densities. The charge accumulation on the dielectric and the voltage boundary conditions for dielectrics have been derived by considering an equivalent circuit of the gas gap in series with the equivalent capacitor of the dielectric. Complications in modeling the dielectric barrier discharge are generally related to the complexity of reactions in the ionization layer and randomness of the discharge regime in some configurations. In order to overcome these problems, a single species DBD model for a point to plane configuration is presented in this paper. The Finite Element Method (FEM) was used to solve the governing equations for both the electric field and distribution of unipolar space charge using the COMSOL multi-physics commercial software. The basic characteristics of the discharge, including the total current, electric field distribution, surface charge accumulation, and space charge density distributions are reported. In addition a sensitivity analysis was carried out to show the effect of the voltage frequency and amplitude on the discharge characteristics. In section II, the governing equation and mathematical model for DBD is presented, in section III, the numerical algorithm is described. Simulation results are illustrated in section IV, and finally the conclusions are presented.

II.   MATHEMATICAL MODEL

A.   *Governing Equations*

Fig.1 shows a typical configuration for dielectric barrier discharge in the point to plane geometry.
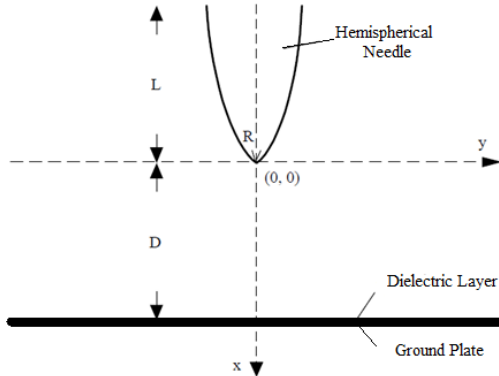
Fig.1. Typical configuration for DBD investigated in this study

A hemispherical needle is perpendicular to an infinitely large plate at a distance D with a tip radius curvature R and length L. A sinusoidal electric potential with the maximum value of V_{max} is applied to the needle. The ambient gas is air at room temperature and atmospheric pressure. As this is a single species model, it is assumed that the ionization layer can be neglected and positive or negative ions with constant mobility are assumed to be injected from the corona electrode. In the absence of magnetic fields, the equations governing the electric field are [11]:

$$\nabla . \vec{D} = \rho \tag{1}$$

$$\nabla . \vec{J} = -\frac{\partial \rho}{\partial t} \tag{2}$$

$$\vec{D} = \varepsilon_0 \vec{E} \tag{3}$$

$$\vec{E} = -\nabla V \tag{4}$$

where $\vec{D}$ is the electrostatic displacement, ρ is the space charge density, $\vec{J}$ is the electric current density, ε_0 is the gas permittivity, $\vec{E}$ is the electric field and V is the electric potential. The electric field is thus governed by Poisson's equation:

$$\nabla^2 V = -\frac{\rho}{\varepsilon_0} \tag{5}$$

The ionic charges are accelerated by the Coulomb force and move towards the ground plates. The charge drift creates an electric current with a density defined as:

$$\vec{J} = \rho \left(\mu \vec{E} + \vec{u} \right) - D \nabla \rho \tag{6}$$

where $\vec{J}(A/m^2)$ is the current density, $\mu(m^2/V.s)$ is the mobility of ions, $D(m^2/s)$ is the ions diffusion coefficient and $\vec{u}(m/s)$ is the gas velocity. Three terms on the right hand side of Eq. (6) are drift, convection and diffusion currents, respectively. D is the

diffusion coefficient and is equal to:

$$D = \frac{k_B T . \mu}{e_0} \tag{7}$$

where k_B is the Boltzmann constant equal to $1.38065 \times 10^{-23} \left(m^2 k_g / s^2 . K \right)$, T is the absolute temperature, e_0 is the electron charge, equal to 1.602×10^{-19} (C).

Since the drift velocity of ions in Eq. (6) is usually about two orders of magnitude larger than the typical velocity of the gas flow, the convective component in the ionic current density can be neglected, so:

$$\vec{J} = \rho \mu \vec{E} - D \nabla \rho \tag{8}$$

Eq. (8) can be substituted into (2) to derive the continuity equation,

$$\frac{\partial \rho}{\partial t} + \nabla . \left(\rho \mu \vec{E} - D \nabla \rho \right) = 0 \tag{9}$$

Therefore, the electric problem of the corona discharge is governed by a set of two partial differential equations with two unknown distributions: Eq. (5) with the unknown potential V and Eq. (9) with the unknown space charge density ρ.

B. *Complementary equations for modeling dielectric barrier discharge*

The main point in simulating DBD is to include surface charge accumulation on the dielectric surface. This surface charge produces a field directed against the electric field due to the voltage source to an extent that the ionization eventually stops. To include this choking action of the dielectric barrier it is necessary to introduce an additional boundary condition which can treat charge accumulation at the dielectric surface and the resulting local reduction of the electric field in the discharge gap. As soon as the field falls below the value necessary to sustain ionization the discharge ceases. The critical interface boundary condition for DBD is accentuated by the dominant electrical field. The surface charge accumulation plays a controlling role for the self-limiting feature of DBD for transition from discharge to spark. According to Maxwell equations, the tangential and normal components of the electrical intensity and electrical displacement at the interface of air and dielectric material must satisfy the following conditions [12]:

$$\vec{n} \times \left(E_d - E_a \right) = 0 \tag{10}$$

$$\vec{n} \times \left(D_d - D_a \right) = \rho_s \tag{11}$$

In the above equations, the subscripts *d* and *a,* correspond to dielectric or air. The time derivative of surface charge density is related to the normal current density:

$$\frac{\partial \rho_s}{\partial t} = \vec{n} . \vec{J} \tag{12}$$

The current density $\vec{J}$ is defined in Eq. (8), so, the surface charge accumulation is calculated by:

$$\rho_s = \int J_n.dt + C_0 \tag{13}$$

C. Boundary Conditions

The boundary conditions for the potential are very straightforward: a given electric potential (V_{ap}) on the corona electrode and zero on the ground plane [13]:

$$V = V_{ap} \text{ on the corona electrode,}$$
$$V = 0 \text{ on the ground plate.}$$

The value of space charge density at different points of the corona electrode is the only required boundary condition for space charge density. However, formulation of proper boundary conditions for the space charge density is not so easy because the ionization layer has been neglected. One possible approach is to use Kaptzov's hypothesis, which can be used to create a simple algorithm, which helps to establish the charge injection law. Kaptzov suggested that if the corona discharge occurs at some point on the electrode and charge is injected, the electric field at this point remains at the value it takes at the corona onset.

The potential of the electrode at the point where the very first time charge is injected to the domain defines the corona onset level, and the corresponding value of the electric field will be the critical electric field, which remains nearly constant during the discharge. In highly symmetrical arrangements of electrodes, for example hemispherical ones, there exists an analytical solution for the onset electric field. The result is known as Peek's equation and in air it has the following form:

$$E_0 = 3.1 \times 10^4 \delta \left(1 + \frac{0.308}{\sqrt{0.5\delta R}} \right) \tag{14}$$

where $\delta = T_0 P / TP_0$, R is the electrode radius in *cm*, T_0 the standard temperature, T the actual temperature, P_0 the standard pressure and P the actual pressure of gas. It must be emphasized that Peek's equation can be used only, if the electric field is the same at all points of the discharge electrodes.

The values of the charge density should be selected in order to satisfy the Kaptzov condition. The electrode tip has a spherical shape, but the electric field is not constant and slightly varies from one point of the surface to another. Formally speaking the corona onset voltage and critical electric field would have to be different at all points. However, for the simplification of the algorithm, a constant critical electric field has been assumed. The initial density of the space charge has to be guessed, or taken from a previous solution at similar conditions. After the problem is solved the electric field on the electrode surface is compared with Peek's value and the electric charge updated. While some well-founded techniques are often advised the following simple formula proved to be very effective [13]:

$$\rho_{new} = \rho_{old} + \beta \times (E - E_0) \tag{15}$$

where β is an experimentally found constant. Practically speaking, this approach provides an indirect boundary condition for space charge density. Its distribution on the corona electrode surface is iterated until the corona electrode electric field is sufficiently close to Peek's value.

<div align="center">III. Numerical Algorithm</div>

The processes occurring in the dielectric barrier discharge during a cycle of AC voltage are more complicated than that for a corona discharge. By applying an electric field larger than the breakdown field local ionization in the gap is formed, which initiates the current in the domain. During the positive half cycle this current causes negative ions to deposit on the needle, and positive ions to accumulate on the dielectric. So, the total electric field intensity is a combination of the electric field produced by the voltage source and the field produced by the space charge collected on the dielectric surface. As the discharge progresses the charge accumulated on the dielectric surface reduces the local electric field to such an extent that ionization stops and the current is choked. When the sign of voltage reverses, the source field reinforces the field due to surface accumulation. This enhanced field at the beginning of the new half cycle initiates a new current, which transfers charge to the dielectric surface until the opposing space-charge field once again extinguishes the ionic current across the gap [14].

Following this description, a numerical algorithm for the dielectric barrier discharge simulation was developed. The algorithm for solving the space charge density follows an iterative approach. The simulation starts from some initial guess of the space charge density, and then the conventional FEM procedure is employed to obtain the Poisson component of the electric potential in Eq.(5) while a high voltage is applied to corona needle and the ground plate is kept at zero potential. After calculating V, the electric field is calculated by differentiating the potential distribution. Using the values of electric field, the new charge density distribution is obtained by solving Eq. (15). This process continues and the iterative algorithm updates the injected charge density on the corona electrode surface until the electric field values are sufficiently close to Peek's value. Finally, all local parameters of the electric dielectric barrier discharge, including the space charge density, the current density, the electric field and the potential for every point in the simulation domain can be obtained. It should be noted that the electric field varies strongly in both space and time. Near the discharge electrode the electric field variation is particularly steep which demands a very fine spatial mesh, while in the remaining region the electric field variation is more uniform. A non-uniform spatial mesh is therefore essential for an accurate numerical treatment near the electrodes and the air gap. In addition, the numerical algorithm for determining space charge density should fulfill few requirements [11]. It should give positive, accurate results, free from nonphysical density fluctuation and numerical diffusion, should be computationally efficient, and should be easily adopted for any geometry.

A. Current

The formula for the discharge current induced due to the motion of ions between electrodes has been derived from an energy balance equation. In this study, a formula for the discharge current is derived for general electrode geometry from the energy balance equation in which the displacement current is explicitly taken into account. $\vec{E}$ is electric field modified by the space charge:

$$\vec{E} = \vec{E_s} + \vec{E'} \tag{16}$$

where $\vec{E_s}$ is the static applied field without effect of charge transport and $\vec{E'}$ is the field produced by the space charge. It is already assumed that this study is based on single species model without the effect of electrons. By doing few simplifications the current equation could be calculated as follow [15]:

$$I = \frac{1}{V_{ap}} \iiint \rho\mu \, \vec{E'}.\vec{E_s} \, dv \tag{17}$$

The sinusoidal voltage (V_{ap}) was defined based on the following equation:

$$V_{ap} = V_{max} \sin(2\pi f t)$$

Fig. 2 shows the distribution of electric field intensity on the tip of the needle for different time steps. As it is obvious for all the times and voltages, the maximum value for electric field intensity is close to Peek's value of $1.623 \times 10^7 \, (V/m)$.
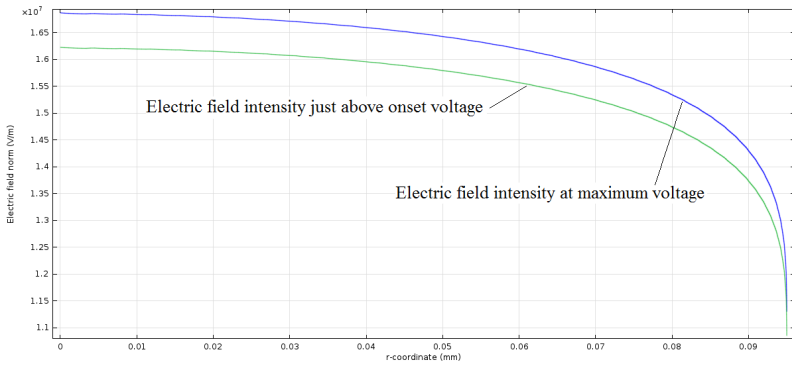
Fig.2. Electric field intensity on the tip of needle for different values of voltage above onset with effect of charge injection

To have a better understanding of this issue, distribution of the electric field intensity on the tip of the needle without injecting the charge (the Laplace equation) is shown in Fig. 3. The main point in Fig. 3 is that for Laplacian model the maximum electric field intensity is a function of the applied voltage. A larger value of the applied voltage results in a greater value for electric field.
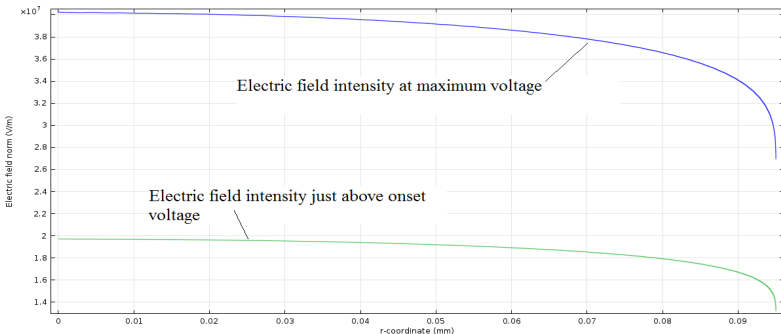

Fig.3. Electric field intensity on the tip of needle for different values of voltages above onset without effect of charge injection

IV.   SIMULATION RESULTS

In this study, a hemispherical needle *L=1cm*, is placed perpendicular to the aluminum plate with *25 cm* radius at the distance *D = 3.1cm*. The radius curvature *R* of the tip of the needle is *95µm*. A dielectric layer with thickness of *1mm* is assumed to be placed on the ground plate, and the relative permittivity of this material is *6*. At the room temperature and atmospheric pressure the corona onset voltage for this configuration is evaluated to be *3.1kV*. The high voltage supplied to the needle varied between the corona onset level and *8 kV*. The frequency of the basic model is *5 kHz*.

The first simulation was done for the maximum input voltage of *7.5 kV* and the frequency of *5 kHz*. Total corona current between both electrodes and the distribution of the charge density on the ground plate were calculated. The waveform of injected voltage is shown in Fig. 4.
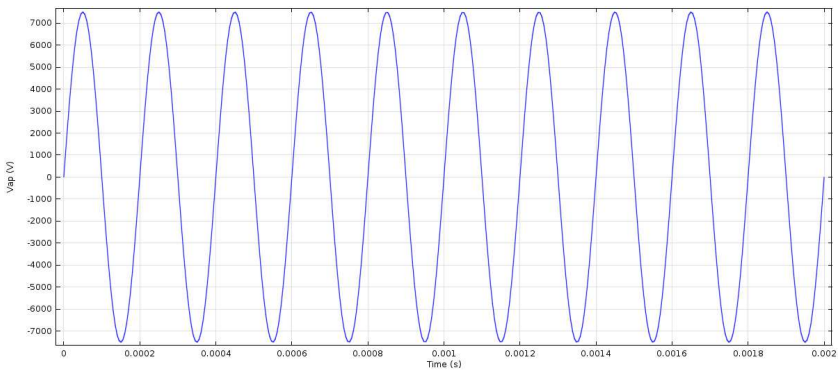
Fig.4. Applied voltage

Fig. 5 shows the distribution of the electric field intensity with and without the effect of accumulated charges in space and on the surface of the dielectric:
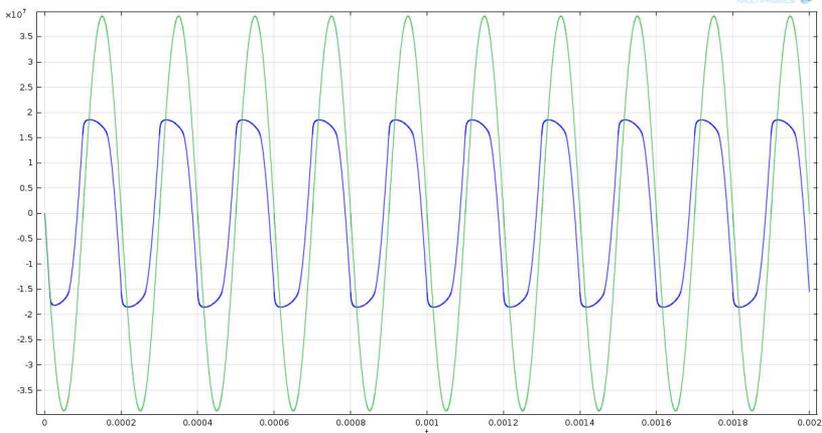

Fig.5. Electric field intensity with and without effect of injected charge on the needle's tip

Two observations are dominant in the figure above. First, the electric field is distorted due to effect of injected space charge from the tip of the needle and the accumulated surface charge on the dielectric. The major effect of such distortion at this level of voltage is on

the electric field intensity above Peek's value before voltage zero crossing. So, it was observed that for this level of voltage and frequency the current is shifted with respect to the voltage and it has been shown in Fig. 6:
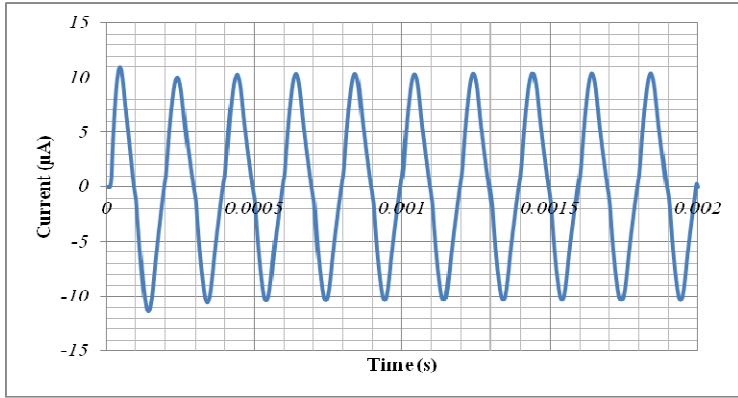

Fig.6. Waveform of the discharge current

The second one is that although the electric field magnitude is not exactly equal to Peek's value at all the points on the needle's tip, but, as stated before, the iterative algorithm is used to modify the injected charge and as a result the difference between the highest value above onset value is very small.

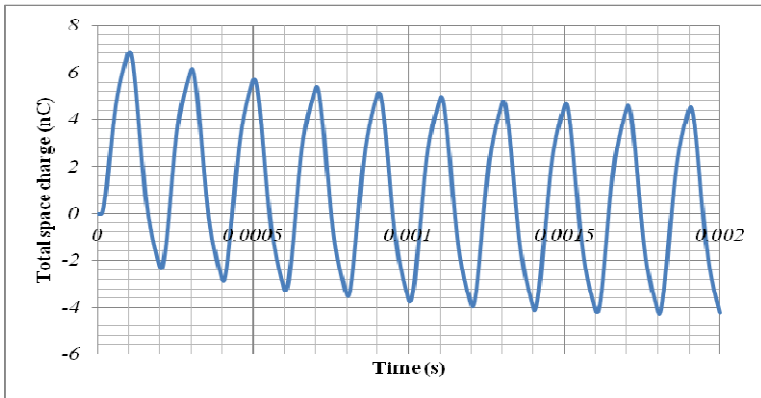In Fig. 7 the total space charge in the air gap is shown as a function of time:

Fig.7. Distribution of space charge in the air gap

In first positive half cycle since there is no charge in the system, there is a short time delay before the charge injection occurs to the domain. This charge reaches its maximum and after that the negative ions are injected in the negative half cycle. There is a zero crossing in this figure that shows the net amount of negative and positive ions is equal. This is really important to note that this point does not coincide with the zero crossing in the absorbed current. Also the sign of the current follows the sign of the electric field intensities with and without effect of charge and in a specific point equals to zero. It is obvious that after couple of periods the total space charge in the domain for both negative and positive cycles stabilizes.

By using the surface charge accumulation output from the COMSOL program, and applying the integral on the surface of the dielectric, the total surface charge on the dielectric is shown in Fig. 8.
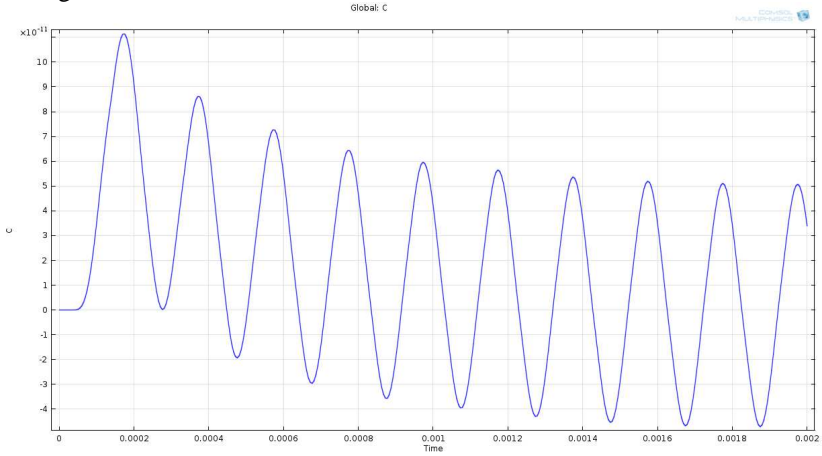

Fig.8. Accumulated surface charge on dielectric layer

Fig. 9 shows the space charge density distribution in the air gap along the axis of symmetry. It is an important note in the model that at high frequencies, the transition time from positive to negative cycle is smaller than the time that is needed for charge transport, so, at some points in the simulation there are negative charges already in the domain and positive charges start to be injected from the needle and vice versa. At a frequency of 50 Hz the importance of this note is not that much, because ions with specific polarity have enough time to settle on the collector before the needle starts to inject ions with opposite polarity on the next half cycle of voltage.
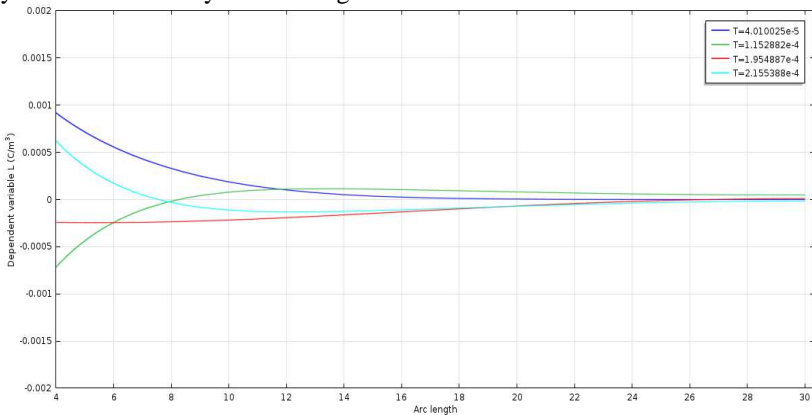

Fig.9. Distribution of space charge along the axis of symmetry

Note that at $t=4.01\times10^{-5}$ (s) (the positive half-cycle) just positive ions in the domain exist. For other values (for example $t=1.15\times10^{-4}$ (s), and $t=2.15\times10^{-4}$ (s)), both positive and negative are present. For $t=1.95\times10^{-4}$ (s) negative ions are dominant.

If all the parameters are kept the same as previous model but the level of voltage changes to lower values ($V_{max} = 3.2\ kV$) which is around the onset voltage, the shape of current is shown in Fig 10.
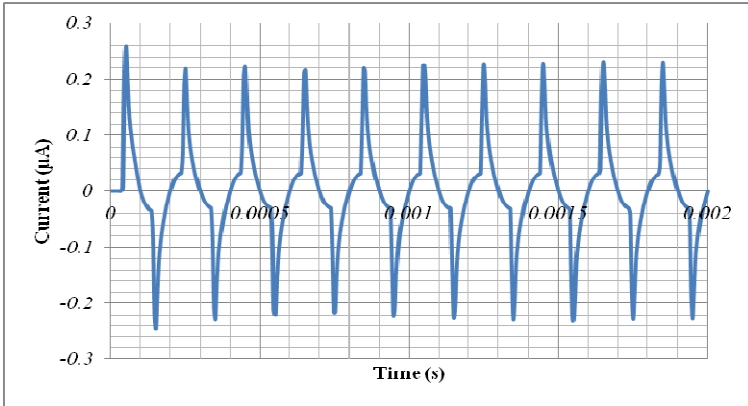

Fig.10. Shape of current just above onset voltage at 5 kHz

This figure is very interesting, as the maximum voltage is just above onset level, so, after the voltage goes above the onset a small amount of charges are injected to the domain, and after that injection stops. As a result, current starts to decrease and the convection current still continues until the next half cycle when there is a charge injection in the opposite direction. Fig. 11 shows the total space charge for the above case:
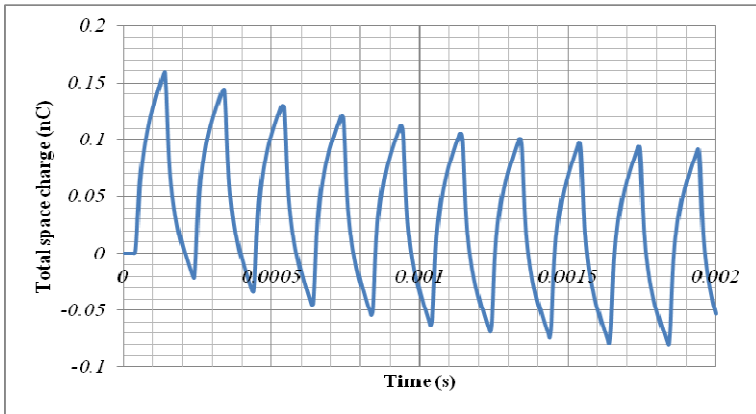

Fig.11. Total space charge in domain just above onset voltage at 5 kHz

As it is shown the shape of the total charge in the domain is nearly the same as the basic model, but the maximum value for positive and negative ions after few cycles is few times less than the previous case. For $V_{max}=3.2\ [kV]$, and frequency *50 Hz* the simulation results are shown in Fig. 12.
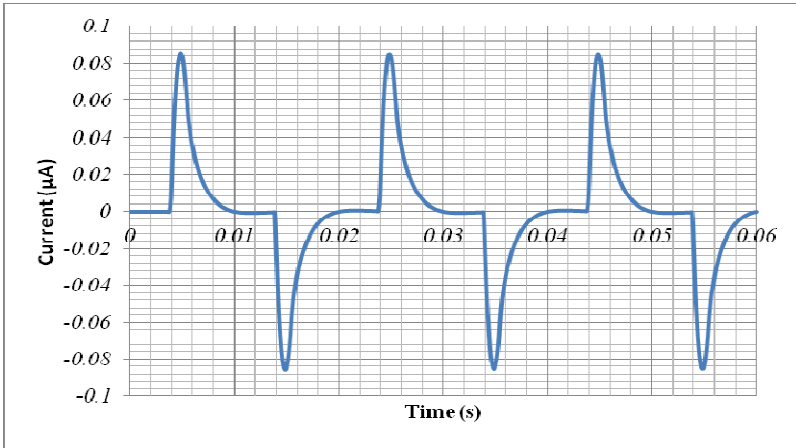
Fig.12. Shape of current just above onset voltage at 50 Hz

Here there is charge injection, and some current in the domain. However after the field at the tip falls below the onset value there is only convection current in the domain and the charge has enough time to be all absorbed by the dielectric layer. Here, almost all the charges in the domain are accumulated on the surface before the needle starts to inject charge in next half cycle voltage. In Fig. 13 the shape of total charge in domain is shown. Two differences are observed in this one in compared to the two previous cases. First of all the settling time, in this case is almost one cycle, and the second one is about the sign of space charge in domain. As it has been shown, in positive half cycle, positive ions are injected to the domain, after the point that voltage drops below onset voltage, up to the next half cycle, all charges in domain have enough time to accumulate on the dielectric layer and there is almost no charge with opposite sign in the domain. Because of this the current rises abruptly and then decays, and at some points in the cycle there is no charge in the system to produce current, and the current drops to zero.
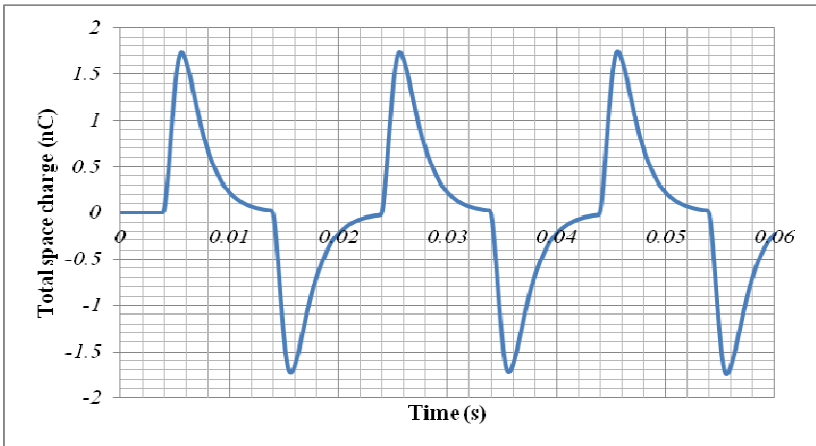

Fig.13. Total space charge just above onset voltage at 50 Hz

Fig. 14 shows the variation of the total space charge and maximum current at the fixed frequency and for different level of voltages. As was expected at the voltage levels below the onset voltage almost there is no charge injection and as a result there is no current in domain. But when the voltage is increased above the onset level the total corona current increases faster than linearly with the voltage. The total charge curve is almost linear.
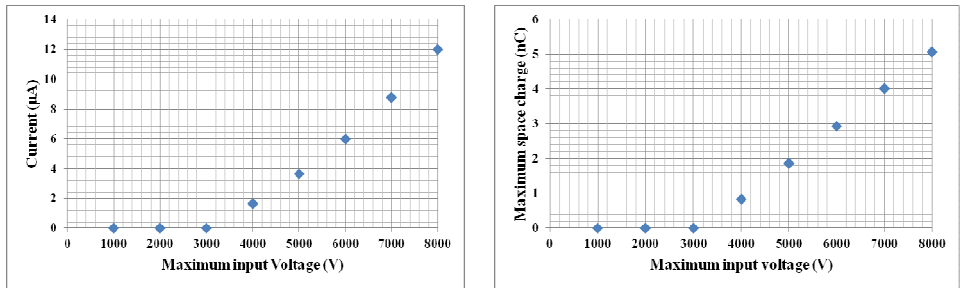

Fig.14. Maximum current (left hand side) and maximum space charge (right hand side) in domain at different voltages and at 5 kHz

Fig. 15 shows the variation of the total space charge and maximum current at the fixed voltage and for different level of frequencies. As the level of frequency goes up, the current level increases due to the fact that transition time from positive cycle to negative cycle gets smaller and continuous clouds of positive and negative ions are going to be formed. But, the net charge in whole domain is smaller at higher frequencies, because at lower frequencies ions with the same polarity are dominant in a half cycle, and starting from following cycle almost all the ions are settled on dielectric layer.
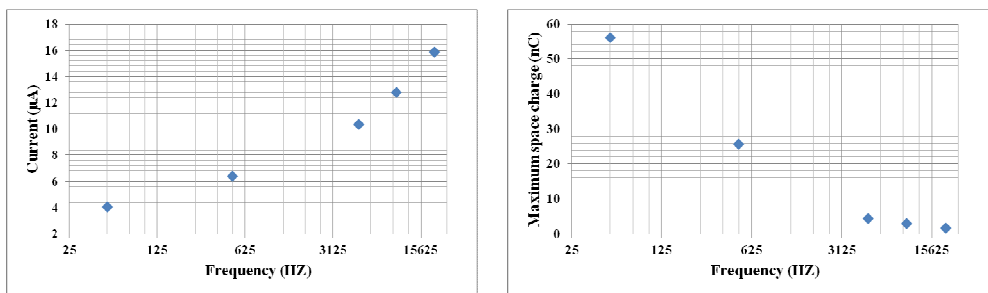

Fig.15. Maximum current (left hand side) and maximum space charge (right hand side) in domain at different frequencies and at 7.5 kV

V.   CONCLUSIONS

In this paper, a quasi-stationary single-species FEM model for simulating the dielectric barrier discharge has been proposed. The governing equations considering the effect of surface charge accumulation was developed. For the charge transport model a partial differential equation with the effect of diffusion coefficient was employed and artificial diffusion has been added to obtain a stable algorithm. The main objectives of this study are the investigation on the electrical behavior of the system including electric field in-

tensity, space charge distribution, surface charge accumulation, and total absorbed current. Sensitivity analysis of voltage and frequency level has been carried out in order to investigate the time variation of the discharge. The results show the behavior of the corona current and space charge density for sinusoidal voltage at different frequencies and voltage levels. In the basic model, the current shifting in a system with a dielectric barrierl was shown based on the effect of the reverse electric field produced by surface charge accumulation. Also it was shown that for higher frequencies a combination of positive and negative ions have contributions on to the current generation. In this study the shape of the current waveform for both positive and negative voltage half cycles have the same shape because of the fact that this is based on the single species glow dielectric discharge. So, there is no sign of fast rise Trichel like pulses in the negative half cycle. By sensitivity analysis on the voltage level, it was also shown that as expected, larger input voltage results in a larger current in the circuit. The average current depends on the frequency as well and increases as the frequency of input voltage increases.

REFERENCES

[1] Ulrich Kogelschatz, Dielectric-barrier Discharges: Their History, Discharge Physics, and Industrial Applications, Plasma Chemistry and Plasma Processing, Vol. 23, No. 1, March 2003.

[2] B. Eliasson, U. Kogelschatz, Non-equilibrium Volume Plasma Chemical Processing, IEEE Transaction on Plasma science, Vol. 19, No. 6, December 1991.

[3] Ulrich Kogelschatz, Filamentary, Patterned, and Diffuse Barrier Discharges, IEEE Transactions on Plasma Science, Vol. 30, No. 4, August 2002.

[4] S. Kanazawa, M. Kogoma, T. Moriwaki, S. Okazaki, Stable glow plasma at atmospheric pressure, Journal of Physics D: Applied Physics Vol. 21, No. 5, 1988.

[5] L. Yang, Y. Hao, E. Tu, X. Wang, J. Chen, Mechanism and Characteristic of Dielectric Barrier Multipulse Glow Discharge in Helium at Atmospheric Pressure, Proceedings of the 9th International Conference on Properties and Applications of Dielectric Materials, July 2009.

[6] R. Gouri, N. Zouzou, A. Tilmatine, L. Dascalescu, Enhancement of submicron particle electrostatic precipitation using dielectric barrier discharge in wire to square tube configuration, Journal of electrostatic, 2012.

[7] B. Dramane, N. Zouzou, E. Moreau, G. Touchard, Electrostatic precipitation of submicron particles using a DBD in axisymmetric and planar configurations, IEEE transactions on Dielectrics and Electrical Insulation, Vol. 6, No. 2, April 2009.

[8] H. Tsubone, J. Ueno, B. Komeili, S. Minami, G.D. Harvel, K. Urashima, C.Y. Ching, J.S. Chang, Flow characteristics of dc wire-non-parallel plate electro-hydrodynamic gas pumps, Journal of Electrostatics, September 2008.

[9] J.S. Chang, H. Tsubone, Y.N. Chun, A.A. Berezin, K. Urashima, Mechanism of eletrohydrodynamically induced flow in a wire-non-parallel plate electrode type gas pump, Journal of Electrostatics, 2009.

[10] F. Massines, A. Rabehi, P. Decomps, R. B. Gadri, P. Ségur, C. Mayoux, Experimental and theoretical study of a glow discharge at atmospheric pressure controlled by dielectric barrier, J. Appl. Phys., 1998.

[11] P. Sattari, G.S.P. Castle, K. Adamiak, FEM-FCT Based Dynamic Simulation of Corona Discharge in Point-Plane Configuration, Conf. Presentation – P1.17

[12] J. S. Shanga, P. G. Huang, Modeling of ac dielectric barrier discharge, Journal of Applied Physics, June 2010.

[13] K. Adamiak and P. Atten, "Simulation of corona discharge in point-plane configuration," J. of Electrostat., vol. 61, 2004.

[14] W. Breazeal, K. M. Flynn, and E. G. Gwinn, Static and dynamic two-dimensional patterns in self-extinguishing discharge avalanches , Physical Review, Vol. 52, No. 2, August 1995.

[15] N. Sato, Discharge current induced by the motion of charged particles, J. Phys. D: Appl. Phys., 1980.